

We are IntechOpen, the world's leading publisher of Open Access books Built by scientists, for scientists

5,800

Open access books available

142,000

International authors and editors

180M

Downloads

Our authors are among the

154

Countries delivered to

TOP 1%

most cited scientists

12.2%

Contributors from top 500 universities



WEB OF SCIENCE™

Selection of our books indexed in the Book Citation Index
in Web of Science™ Core Collection (BKCI)

Interested in publishing with us?
Contact book.department@intechopen.com

Numbers displayed above are based on latest data collected.

For more information visit www.intechopen.com



Chapter

Some New Progress in the Experimental Measurements on Electrical Property of Main Minerals in the Upper Mantle at High Temperatures and High Pressures

Lidong Dai, Haiying Hu, Yu He and Wenqing Sun

Abstract

In this chapter, we present the recent progress in the experimental studies of the electrical conductivity of dominant nominally anhydrous minerals in the upper mantle of the deep Earth interior, namely, olivine, pyroxene, and garnet. The influences from pressure, oxygen partial pressure, and anisotropic orientation on hydrous and anhydrous electrical conductivities of minerals and rocks have been already explored detailedly. There are two main electric conduction mechanisms in Fe-bearing mantle minerals, for example, small proton and proton hopping conditions, which are well distinguished by the magnitude of activation enthalpy at high temperature and high pressure. Likewise, the conduction mechanisms are efficiently characterized by these obtained positive and negative effects from the oxygen fugacity on electrical conductivities of corresponding dry and wet Fe-bearing silicate minerals at the regions of the upper mantle under conditions of different oxygen partial pressures. On the base of high-pressure laboratory-based conductivity measurements for these nominally anhydrous minerals (e.g., olivine, pyroxene, and garnet), the water content will be estimated within the depth range of the upper mantle. In comprehensive considerations of filed geophysical magnetotelluric results, the electrical conductivity measurements of dominant upper-mantle minerals can thoroughly disclose the distribution, storage state, and migration conduction in the deep Earth interior.

Keywords: electrical property, upper-mantle minerals, water content, oxygen fugacity, high temperatures and high pressures

1. Introduction

Global and regional field magnetotelluric (MT) and geomagnetic deep sounding (GDS) results revealed that there existed many high electrical conductivity layers

(HCL) in various geotectonic units in the deep Earth's interior (the magnitude of electrical conductivity range is 10^{-2} – 10^0 S/m) [1, 2]. To investigate the cause of all of these available high conductivity layers, it is crucial to measure the electric transport properties of minerals and rocks at certain high-temperature and high-pressure conditions. As one of the crucial physical parameters of minerals, electrical conductivity (EC) is highly sensitive to temperature, pressure, and depth, which is strongly dependent on the physical and chemical environments in the deep Earth and other planetary interiors [3–5]. In particular, EC is dependent on several factors such as diffusion coefficients of alkali ion [6, 7], trace elemental contents [8], the spin transition of the electron [9, 10], anisotropic crystal orientation [11–15], contents of water and other volatile elements [16–18], partial melting [19–21], dehydration (or dehydrogenation) effects of minerals [22–24], impurity of high-conductivity phase [25, 26], salinity-bearing (or water-bearing) fluids [27, 28], and structural phase transformation (amorphization or metallization) [29–34].

In the recent 20 years, with the development of measuring techniques and experimental methods of electrical conductivity in the AC electrical impedance spectroscopy (EIS) technique and multi-anvil high-pressure apparatus, there is a large number of research results on the electrical properties of minerals and rocks to be reported in the upper-mantle and mantle transition zone. Some international famous research administrations have successfully set up the experimental platform and measurement system of minerals and rocks at high temperatures and high pressures, such as the Key Laboratory of High-temperature and High-pressure Study of the Earth's Interior (HTHPSEI), Institute of Geochemistry, Chinese Academy of Sciences, the People's Republic of China; the Karato High-pressure Laboratory, Department of Earth and Planetary Sciences, Yale University, United States; the Laboratoire Magmas et Volcans, Université Clermont Auvergne, French National Centre for Scientific Research, France; the Scripps Institution of Oceanography, University of California San Diego, United States; University of Bayreuth, Germany; and Okayama University, Japan.

As we know, previously available classic “Pyrolite” mineralogical models have already confirmed that the nominally anhydrous minerals (NAMs, e.g., olivine, pyroxene, and garnet) are dominant mineralogical composition in the upper mantle of the deep Earth interior. In light of the FTIR result, these NAMs can contain a certain amount of structural water rather than absolutely “dry.” Whereas, it is general that the trace structural water in NAMs stably exists as a form of hydroxyl point defect of the crystalline site in these minerals. Due to the presence of trace structural water in NAMs, many physical and chemical properties of NAMs have been thoroughly changed accordingly, such as electrical conductivity [3, 8, 13–18, 35], diffusivity [36, 37], plastic deformation [38, 39], seismic wave attenuation [40, 41], grain growth [42, 43], and kinetic recrystallization [44, 45]. In the world, by virtue of the theoretical calculations of Nernst-Einstein equation between the electrical conductivity and coefficient in mineral, Professor Shun-ichiro Karato from the Karato High-pressure Laboratory, Department of Earth and Planetary Sciences, Yale University, United States firstly brought forward the viewpoint that the trace structural water in hydrous olivine can enhance several orders of magnitude in the EC of upper-mantle mineral, which can be used to reasonably explain the observed high conductivity anomaly in the region of asthenosphere [46]. In the following 20 years, as a research hotspot in the field of solid Earth science, a large amount of research work of electrical conductivity of minerals and rocks from the laboratory high-pressure experiments and theoretical calculations investigated have been conducted to focus on this hypothesis of

water for the NAMS in the upper-mantle zone (olivine: [8, 13–15, 47–50], pyroxene: [51], and garnet [52–54]). In the year 1998, it is first that Xu Yousheng from the Bayerisches Geoinstitut, University of Bayreuth, Germany fetched in AC electrical impedance spectroscopy (EIS) technique and applied it to report a series of electrical conductivity of minerals, such as olivine, orthopyroxene, and garnet of the upper mantle; wadsleyite of mantle transition zone; as well as the silicate perovskite of the lower mantle under conditions of high temperatures and high pressures in the multi-anvil high-pressure apparatus [55–60]. Generally, to explore the effect of water on the electrical conductivity, we need to obtain a series of starting materials of hydrous either hot-pressure sintering synthetic or natural hydrous samples. Then, at a fixed temperature and pressure condition, we can measure the electrical conductivity of hydrous minerals. Further, the functional relationship between the EC and water content can be established at HP and HT conditions, thereby providing constraints of the water content in the deep Earth's and planetary interiors.

In this chapter, we reviewed some recent progress in the electrical conductivity of the main NAMS in the region of the upper mantle, that is, olivine, pyroxene, and garnet at conditions of high temperatures and high pressures. Then, some experimental methods, measurement techniques, and electrical transport conduction on the electrical conductivity of minerals are summarized in the multi-anvil high-pressure apparatus. The newest progress in the recently reported conductivity measurements is outlined in detail. Finally, some comprehensive remarks on the mineral electrical conductivity are discussed.

2. Electrical conductivity of upper-mantle minerals

The electrochemical AC impedance spectroscopy is the most efficient method to measure the electrical conductivity of minerals and rocks at HT and/or HP conditions [61–64]. The AC signal voltage and scanning frequency need to be designated before the sample resistance is measured. As usual, for a special mineral single specimen, the electrochemical AC impedance spectroscopy of samples consists of grain boundary impedance arc, and as well as the interface impedance between sample and electrode. However, for a special polycrystalline aggregate or rock, the electrochemical AC impedance spectroscopy of samples consists of grain boundary impedance arc, grain boundary impedance, and the interface impedance between sample and electrode. For each individual complex impedance spectroscopy, there are four parameters to be obtained at the same time, for example, real part, imaginary part, magnitude, and phase angle at the same time. The relation can be expressed as,

$$Z_r = |Z| \cos \varphi \quad (1)$$

$$Z_i = |Z| \sin \varphi \quad (2)$$

Here, Z_r stands for the real part of complex impedance spectroscopy, Z_i stands for the imaginary part of complex impedance spectroscopy, $|Z|$ stands for the magnitude of complex impedance spectroscopy, and φ stands for the phase angle of complex impedance spectroscopy. Representative complex impedance spectra for natural eclogite from the Dabie-Sulu ultrahigh-pressure metamorphic belt of eastern China are shown in **Figure 1**.

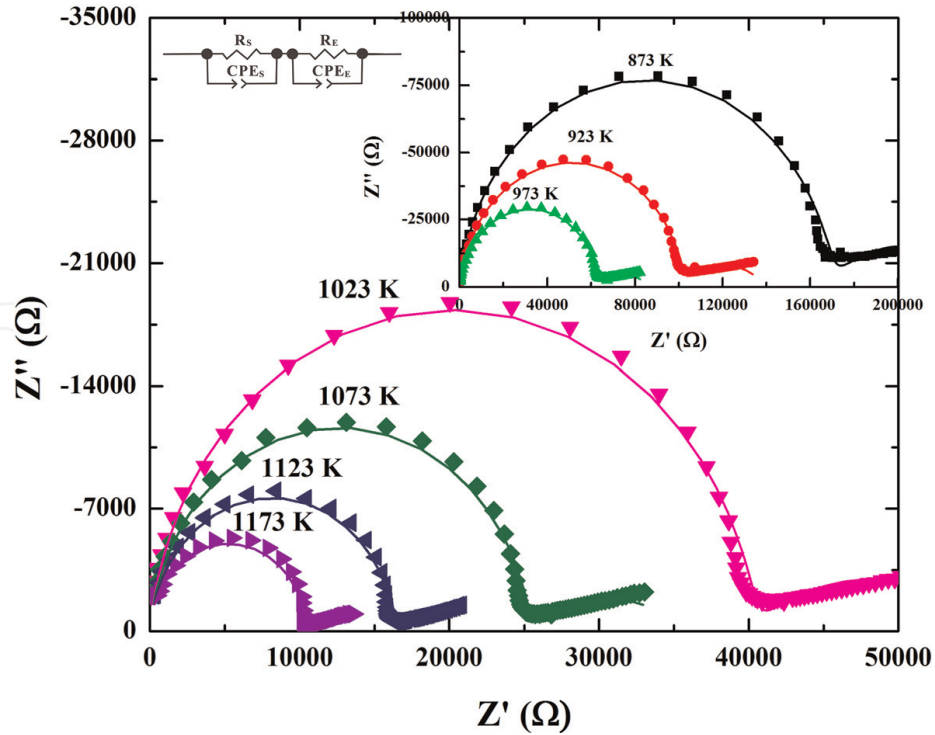


Figure 1. Representative complex impedance spectra for natural eclogite from Dabie-Sulu ultrahigh-pressure metamorphic belt of eastern China at conditions of 3.0 GPa, 873 K–1173 K and frequency range of 10^{-1} – 10^6 Hz (reproduced with permission from Dai et al., *Geochem. Geophys. Geosyst.*; published by American Geophysical Union, 2016 [4]).

Detailed description of measurement theory and experimental method of impedance spectroscopy are given in our previous review chapter [9]. The equivalent electric circuit was selected to fit the impedance spectroscopy of the sample, which is composed of some fundamental electronic elements (e.g., resistor, capacitor, inductor, constant phase element (CPE), Gerischer element, Warburg element, etc.) [65–68]. After that, the electrical conductivity of the sample was obtained by the sample resistance, the calculating formula is expressed as,

$$\sigma = \frac{1}{\rho} = \frac{L}{(R \times S)} \quad (3)$$

In here, σ stands for the electrical conductivity (S/m), ρ stands for the electrical resistivity (m/S), L stands for the sample height (m), and S stands for the cross-sectional area (m^2). At a given pressure condition, it is usual that the electrical conductivity of sample and temperature satisfies with an Arrhenius relation, namely,

$$\sigma = \sigma_0 \exp\left(-\frac{\Delta H}{kT}\right) \quad (4)$$

In here, σ_0 stands for the pre-exponential factor (S/m), ΔH stands for the activation enthalpy (eV), k stands for the Boltzmann constant and T stands for temperature (K).

3. High-pressure apparatuses for conductivity measurements

In the recent several years, many researchers developed the high-pressure electrical property experiments of minerals and rocks by virtue of various high-pressure

experimental apparatuses. From lower to higher pressure conditions, some typical high-pressure apparatuses on the laboratory-based electrical conductivity measurements are mainly included autoclave, piston-cylinder, multi-anvil press, and diamond anvil cell. In this counterpart, we focus on two types of multi-anvil apparatuses—(i) YJ-3000 t multi-anvil press is equipped in the Key Laboratory of High-temperature and High-pressure Study of the Earth's Interior (HTHPSEI), Institute of Geochemistry, Chinese Academy of Sciences, the People's Republic of China and (ii) Kawai-1000 t multi-anvil Press is equipped in the Karato High-pressure Laboratory, Department of Earth and Planetary Sciences, Yale University, United States.

3.1 YJ-3000 t multi-anvil press

Early on half a century ago, Xie Hongsen and his coworkers successfully set up one multi-anvil press of the YJ-3000 t in the Key Laboratory of HTHPSEI, Chinese Academy of Sciences, People's Republic of China. All of these available high-pressure measurement methods including the direct current, single frequency AC, multi-frequency electrical bridge, and electrochemical AC impedance spectroscopy are widely adopted in the past several years. *In situ* high-pressure EC results on minerals and rocks have been published by many previous researchers using this high-pressure apparatus [69–87]. Dai Lidong and his collaborator [88–91] have developed the HP-HT electrical conductivity platform of minerals and rocks in HTHPSEI, as shown in **Figure 2**. It is composed of three main counterpart pieces of equipment, namely, (a) the pressure-generated apparatus of the YJ-3000 t multi-anvil press; (b) the

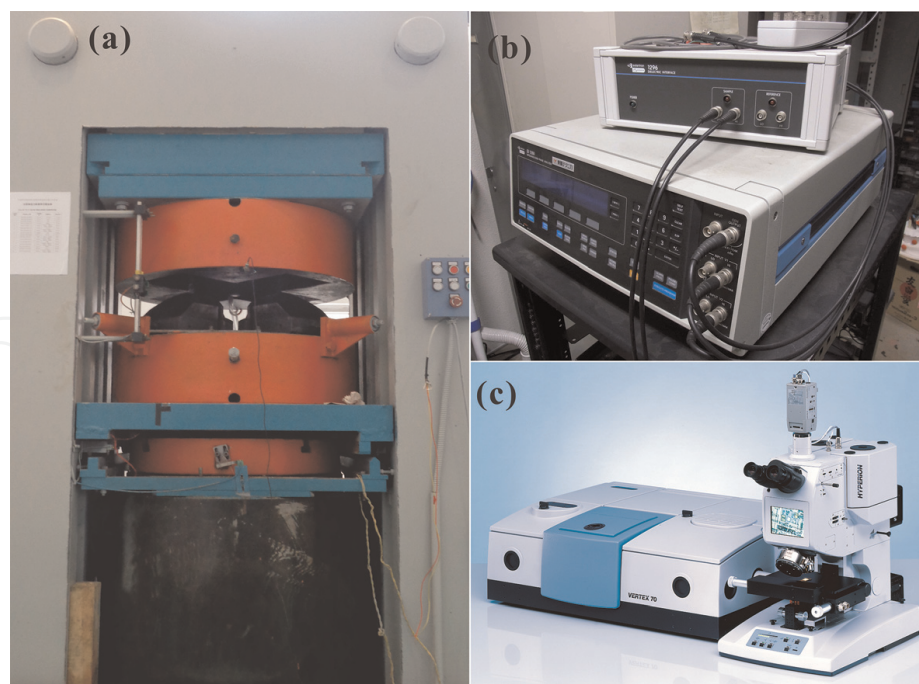


Figure 2. High-pressure conductivity measurement platform and experimental setup in the YJ-3000 t multi-anvil press is equipped in the Key Laboratory of High-temperature and High-pressure Study of the Earth's interior (HTHPSEI), Institute of Geochemistry, Chinese Academy of Sciences, the People's Republic of China. (a) The YJ-3000 t multi-anvil apparatus; (b) the Solartron-1260 and Solartron-1296 interface impedance spectroscopy analyzer operating in the two-electrodes configuration for complex EIS measurements in the frequency range 10^{-4} Hz– 10^7 Hz; (c) the vertex-70v vacuum Fourier-transform infrared spectroscopy (FT-IR) analyzer to check the water content of sample.

Solartron-1260 and Solartron-1296 interface impedance spectroscopy analyzer operating in the two-electrodes configuration for complex EIS measurements in the frequency range 10^{-4} Hz– 10^7 Hz; and (c) the Vertex-70v vacuum Fourier-transform infrared spectroscopy (FT-IR) analyzer to check the water content of the sample. The influential ingredients include temperature, pressure, frequency, oxygen fugacity, water content, iron content, crystallographic anisotropy, grain boundary state, the content of alkali metallic elements, etc. on the electrical characterizations of minerals and rocks have already been explored using this high-pressure conductivity measurement platform in details.

In addition to the *in situ* EC measurements, it has recently become possible to measure some other high pressure-dependent physical properties of minerals and rocks by using the YJ-3000 t multi-anvil press, such as the ultrasonic elastic wave velocity, thermal conductivity, thermal diffusivity, and kinetics of grain growth. [92–100]. Except for wide application in the field of high-pressure mineral physics, the YJ-3000 t multi-anvil press is one of the indispensable tools in some other aspects of high-pressure material science and high-pressure condensed physics.

3.2 Kawai-1000 t multi-anvil press

A representative high-pressure EC experimental assemblage in the Kawai-1000 t multi-anvil press installed in the Karato High-pressure Laboratory, Department of Earth and Planetary Sciences, Yale University, United States [3, 8, 13, 14, 47–49, 51, 52] is displayed in **Figure 3**. Eight cubic WC anvils (it is corresponding to each edge length $26 \times 26 \times 26$ mm³) with the 3–18 mm truncation was adopted to provide a high-temperature and high-pressure quasi-hydrostatic environment. Pressure calibrations were performed by pressure-induced structural phase transformations of some representative semiconducting materials (e.g., pure metallic bismuth, ZnTe, GaP, GaAs,

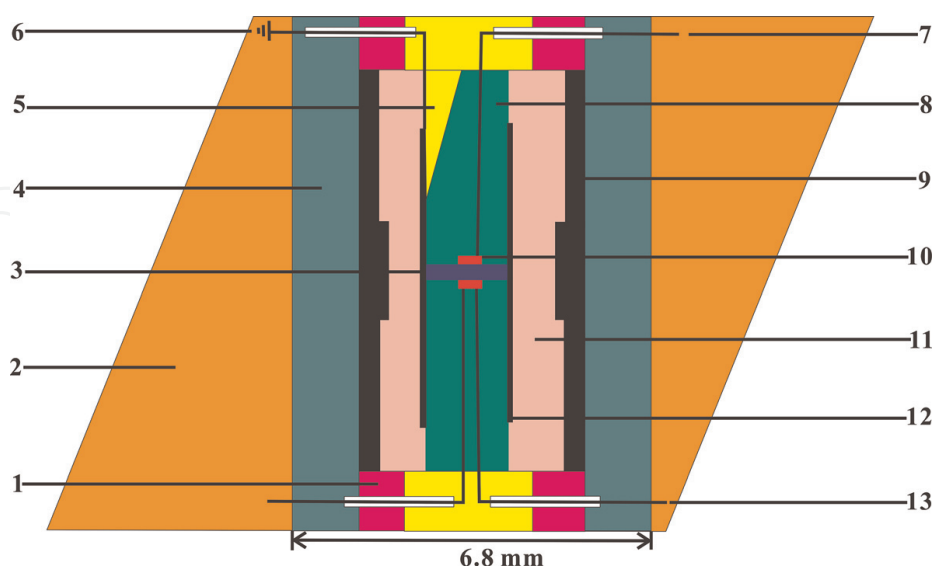


Figure 3.

Sample assembly for the electrical conductivity measurement of minerals and rocks in the Kawai-1000 t multi-anvil press from Shun-ichiro Karato's group from the Karato high-pressure laboratory, Department of Earth and Planetary Sciences, Yale University, United States: (1) metallic Mo ring; (2) MgO octahedral pressure medium with its edge length of 14 mm; (3) sample; (4) zirconia; (5) Al₂O₃ cement; (6) electric grounding; (7) lead wire of metallic electrode and Al₂O₃ insulation tube; (8) insulation tube made of four hole alumina; (9) heater of lanthanum chromite; (10) two symmetric buffer electrodes; (11) MgO insulation tube; (12) metallic shielding case made of Ni, Fe, Re or Mo foil; and (13) thermocouple and Al₂O₃ insulation tube.

etc.) at atmospheric pressure, the structural phase transformation between α -quartz, β -quartz, coesite, and stishovite, and as well as phase transitions between olivine, wadsleyite, ringwoodite, and bridgmanite. The pressure-transmitting medium is made of pure or Cr_2O_3 -doped or Co-doped octahedral magnesium oxide. Two symmetric metallic discs are employed as electrodes of electrical conductivity measurement. A layer of metallic foil was installed to remove the signal disturbance of the measurement electric circuit and environmental noise. As usual, the ordinary heater, such as stainless steel slice, graphite, tantalum slice, and rhenium slice, is reasonably selected on the base of target temperature during a given electrical conductivity measurement. The temperature in the sample chamber is precisely measured by the B-type $\text{Pt}_{70\%}\text{Rh}_{30\%}$ - $\text{Pt}_{94\%}\text{Rh}_{6\%}$ thermocouple or K-type thermocouple. The experimental errors of pressure and temperature are not more than 0.5 GPa and 10 K, respectively.

4. Electrical conductivity of major minerals in the upper mantle

As one crucial cycling of deep Earth interior at the depth range from 80 km to 410 km, the upper mantle mainly contains three main dominant rock-forming minerals, that is olivine, pyroxene, and garnet. Previous available high-pressure experimental results have already confirmed that the electrical conductivity of upper-mantle minerals is highly sensitive to all of these influence ingredients, such as high temperature, high pressure, oxygen partial pressure, trace structural water, iron-bearing content, grain boundary state, graphite layer of grain boundary, magnetite-bearing impurity, titanium-bearing content, chromite-bearing content, sulfur-bearing content, the orientation of crystallographic axis, and partial melting, which is most concerned in the recent several years. Because the crucial effect of water content on EC of minerals and rocks in these representative regions of upper-mantle and mantle transition was neglected by other research groups, in the following paragraph, we mainly pay attention to some related results from Dai Lidong's group from the high-pressure conductivity results from the Key Laboratory of High-temperature and High-pressure Study of the Earth's Interior (HTHPSEI), Institute of Geochemistry, Chinese Academy of Sciences, the People's Republic of China, and as well as Shun-ichiro Karato's group from the Karato High-pressure Laboratory, Department of Earth and Planetary Sciences, Yale University, United States.

4.1 Electrical conductivity of olivine

As a major rock-forming silicate mineral and nominally anhydrous mineral, olivine occupies $\sim 60\%$ of the volume proportion of upper-mantle minerals. Therefore, most of the previously available profile between the electrical conductivity and depth was successfully constructed by the laboratory-based electrical conductivity of olivine data at high-temperature and high-pressure conditions. Electrical conductivities on those of natural olivine single crystal, polycrystalline olivine aggregates, and hot-pressed sintered synthetic olivine have already been performed, especially considering the effects of pressure, oxygen partial pressure, iron-bearing content, and orientation of crystallographic axis on the EC of hydrous olivine.

In an early 1990 year, Roberts and Tyburczy [62] reported the room-pressure electrical conductivity of polycrystalline olivine aggregates using impedance electrochemical impedance spectroscopy (EIS) method under conditions of frequency of 10^{-4} – 10^4 Hz and 1073 K–1673 K. They discussed the influence of anisotropic thermal

expansion-induced porosity and microfracture on the high-temperature electrical conductivity of polycrystalline olivine aggregates. At their measured olivine aggregates with the volume percentage of 2–8% inter- and intra-granular porosity and microfracturing, its effect becomes very feeble for the total electrical conductivity of olivine. In light of their findings, subsequent investigations on the electrical properties of upper-mantle polycrystalline samples do not need to consider the effects of porosity and microcracking. The previous investigation of pressure influence on the EC of olivine single crystal was reported by Xu et al. [55] using the EIS method in the Kawai-1000 t multi-anvil press. Detailed experimental conditions are controlled by pressures of 4–10 GPa, temperatures of 1273–1673 K, frequencies of 10^{-1} – 10^6 Hz, and as well as the solid oxygen buffer of molybdenum and molybdenum dioxide. The acquired pre-exponential factor (σ_0) of ~ 200 S/m, the activation energy (ΔE) of 144.7 kJ/mol and the activation volume (ΔV) of $0.6 \text{ cm}^3/\text{mole}$ are well characterized by fitting Arrhenius relation at upper-mantle temperatures and pressures [60]. A negative pressure-dependent EC of olivine single crystal was also observed, and the electrical conduction mechanism of small polaron hopping between the ferrous and ferric irons of crystalline position was proposed. However, unfortunately, in all of those published results on the EC of olivine and its correspondent high-pressure polymorph in the regions of the upper mantle, mantle transition zone, and lower mantle, Xu et al., did not provide any available information on the water content of the selected experimental samples [55–60].

The first research work for the effect of water on the EC of upper-mantle olivine was found by Karato [46] on the basis of the theoretical calculating of Nernst-Einstein equation, who brought forward that the trace structural water of nominally hydrous minerals plays a vital role in the EC of olivine in the upper mantle. To check this theoretical calculating hypothesis, the EC of hydrous synthetic polycrystalline olivine compacts was firstly conducted by Wang et al. [17] in Shun-ichiro Karato's group from the Karato High-pressure Laboratory, Department of Earth and Planetary Sciences, Yale University, the United States at conditions of a pressure of 4.0 GPa, temperature ranges from 873 K to 1273 K and water content ranges from 100 ppm wt% to 800 ppm wt%, using the Kawai-1000 t multi-anvil press and the Solartron-1260 EIS analyzer (Schlumberger, Houston, TX, USA). It is the first time that the ionized reaction model in hydrous synthetic polycrystalline olivine compacts is originated from the free proton-dominated conduction mechanism, as follows,



where, in the Kröger-Vink notation, $(2\text{H})_M^\times$ represents two hydrogens of crystalline lattice in the position of metallic iron or magnesium, H'_M represents the hydrogen vacancy in the position of metallic iron or magnesium, and H^\bullet represents the free proton.

Furthermore, a series of hydrous electrical conductivity measurements on single-crystal olivine with different crystallographic orientations, synthetic polycrystalline olivine compacts, and synthetic hot-pressed polycrystalline olivine aggregates have been extensively studied by virtue of Kawai-1000 t multi-anvil press and the EIS methods in recent several years [8, 13, 14, 47–49]. **Figure 4** shows the influences of temperature, pressure, oxygen fugacity, iron-bearing content and water-bearing content on hydrous synthetic polycrystalline olivine compacts, and hydrous hot-pressed synthetic polycrystalline olivine aggregates at the temperature ranges from 873 K to 1273 K and pressure ranges from 4.0 GPa to 10.0 GPa.

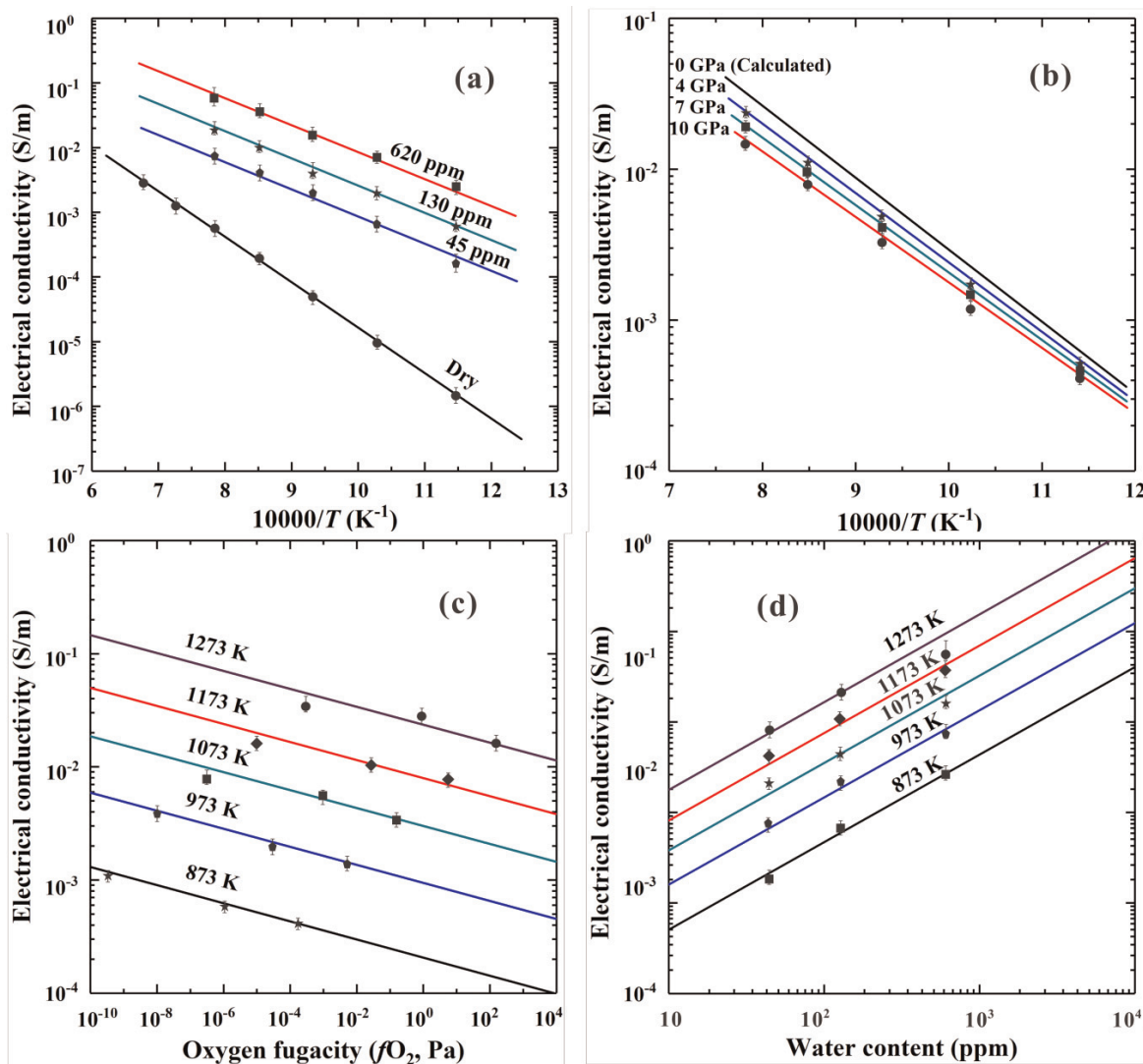


Figure 4. The effects of (a) water content on the EC of X_{Fe} ($Fe/(Fe + Mg)$) = 41.2% hydrous hot-pressed synthetic polycrystalline olivine aggregates, (b) pressure on the EC of hydrous synthetic polycrystalline olivine compacts, (c) oxygen fugacity on the EC of hydrous synthetic polycrystalline olivine compacts, and (d) water-bearing content and temperature on the EC of X_{Fe} ($Fe/(Fe + Mg)$) = 41.2% hydrous hot-pressed synthetic polycrystalline olivine aggregates at the temperature ranges from 873 K to 1273 K and pressure ranges from 4.0 GPa to 10.0 GPa. Three oxygen buffers including Ni-NiO, Mo-MoO₂, and Re-ReO₂ were selected to oxygen fugacity during the process of high-pressure electrical conductivity measurements (reproduced with permission from Dai and Karato, *Phys. Earth Planet. Inter.*; published by Elsevier, 2009 [47–49]).

For hydrous hot-pressed synthetic polycrystalline olivine aggregates with fixed iron-bearing content, X_{Fe} ($= Fe/(Fe + Mg)$) = 41.2% (molar ratio percentage), the electrical conductivity of the sample increases with the rise of water contents from 45 ppm wt% to 620 ppm wt%, and one relatively a fixed activation enthalpy ($\Delta H = 80$ kJ/mole) is observed under conditions of different water contents and temperatures (refer to **Figure 4a** and **d**). The activation enthalpy for hydrous hot-pressed synthetic polycrystalline olivine aggregates is lower than that of the ΔH of dry sample (136 kJ/mole) with the fixed iron content [47]. The influence of pressure on the EC of hydrous synthetic polycrystalline olivine compacts at conditions of 873–1273 K and the oxygen buffer of Ni-NiO controlled oxygen fugacity is displayed in **Figure 4b**. It makes clear that the EC of hydrous synthetic polycrystalline olivine compacts decreases with the pressure increasing from 4.0 GPa to 10.0 GPa, and at the same time, the activation enthalpy and pre-exponential factor of the sample also

reduce, accordingly [49]. **Figure 4c** displays the influence of oxygen fugacity on the EC of hydrous synthetic polycrystalline olivine compacts under conditions of 4.0 GPa, temperatures range from 873 K to 1273 K and fixed water content of 280 ppm wt%. Three oxygen buffers including Ni-NiO, Mo-MoO₂, and Re-ReO₂ were selected to oxygen fugacity during the process of high-pressure electrical conductivity measurements. An available negative electrical conductivity of sample dependence on the oxygen fugacity is observed at each given temperature point at 4.0 GPa, which is attributed to the hydrogen-related defects in hydrous synthetic polycrystalline olivine compacts at conditions of high temperature and high pressure [48]. In all these listed previous cases, the relationship between the logarithm of EC of hydrous (or dry) polycrystalline olivine and the inverse temperature follows a good Arrhenius relation, which is clearly suggesting only one single conduction mechanism controlling the electrical conductivity of hydrous (or dry) sample at high pressure. Furthermore, as pointed out by Dai and Karato [47–49], the dominant conduction mechanisms in the hydrous and anhydrous polycrystalline olivines are corresponding to the hydrogen-related defects (e.g., free proton) and iron-related defects (e.g., small polaron), respectively.

On the other hand, Dai and Karato [13, 14] also measured the EC of hydrous San Carlos single-crystal olivine along with [001, 010, 100] three different crystallographic orientations at conditions of 573–1373 K and 4.0 GPa, as illustrated in **Figure 5** in details. It is clearly observed that at lower temperatures range from 573 K to 900 K, one relatively feeble anisotropic EC in hydrous San Carlos single-crystal olivine with a lower activation enthalpy value ($\Delta H = 74$ kJ/mole) is obtained, which is consistent

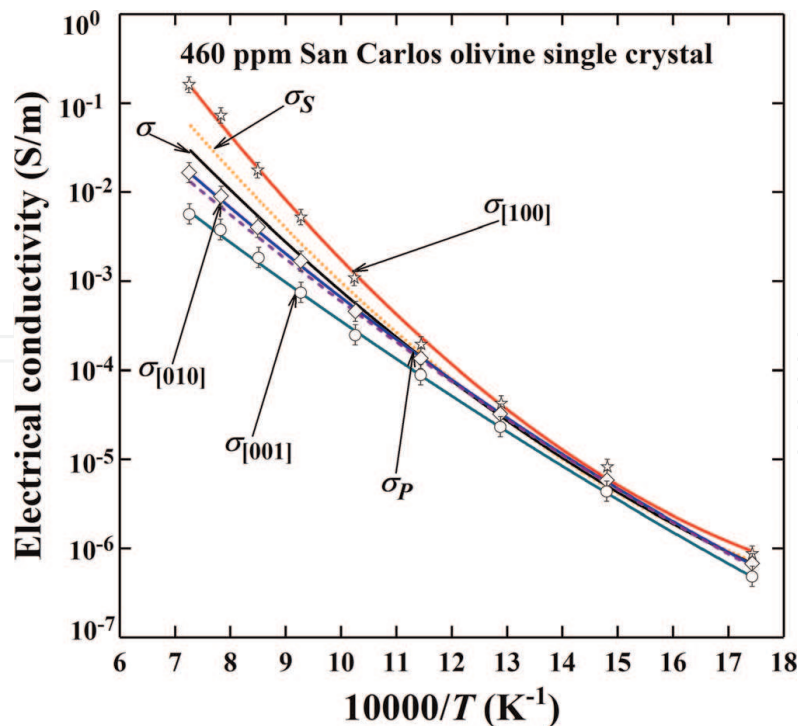


Figure 5.

The influence of anisotropy on the EC of hydrous San Carlos single crystal olivine along [001, 010, 100] three different crystallographic orientations at conditions of 573–1373 K and 4.0 GPa. Three different average schemes of series ($\sigma_S = (\sigma_{[100]} + \sigma_{[010]} + \sigma_{[001]})/3$), parallel ($\sigma_P = 3 \left(\frac{1}{\sigma_{[100]}^2} + \frac{1}{\sigma_{[010]}^2} + \frac{1}{\sigma_{[001]}^2} \right)^{-1}$) and effective medium models ($\langle \sigma \rangle = [\sigma_S + \sigma_P + \sqrt{(\sigma_S + \sigma_P)^2 + 32\sigma_S\sigma_P}]/8$) were applied. (Reproduced with permission from Dai and Karato, *Earth Planet. Sci. Lett.*; published by Elsevier, 2014 [13]).

with previously published EC results [11, 101–103]. In contrast, at a higher temperature ranges from 900 K to 1373 K, the EC of hydrous San Carlos single-crystal olivine with a higher activation enthalpy value ($\Delta H = \sim 130\text{--}150$ kJ/mole) shows an obvious anisotropy along with [001, 010, 100] three different crystallographic orientations, which is in good agreement with the theoretical calculating electrical conductivity results by virtue of high-temperature H–D inter-diffusion method in hydrous single-crystal olivine along with [001, 010, 100] three dominant crystallographic orientations at conditions [104].

In comprehensive considerations of geophysical field observations and geochemical models, the acquired EC results revealed that the high and highly anisotropic EC at the corresponding asthenospheric temperature and pressure conditions is reasonably explained by the high-water content in the region of the asthenosphere (100 ppm). On the other hand, the influence of the interconnected high conductive impurity phases (graphite, magnetite, chromite, sulfide impurity, etc.) and saline fluids (e.g., Ol-NaCl-H₂O, Ol-KCl-H₂O, Ol-CaCl₂-H₂O, etc.) on the EC of olivine has been also explored in details [25–28, 105–107].

Except for high-pressure experimental measurements on the electrical conductivity of hydrous olivine, some important progress from the first-principles calculations based on density functional theory (DFT) has already been performed in order to deeply explore the microscopic electrical transport conduction within an atomic scale in the deep Earth interior. Recently, He et al. [15] firstly designed several point defect models (e.g., $(2H)_{Mg}^{\times}$, $(4H)_{Si}^{\times}$, $[(Fe)_{Mg}^{\bullet}(H)_{Mg}']^{\times}$, etc.) by using the ab-initio molecular dynamics (AIMD) method, and applied them to efficiently provide a robust constraint on different contributions of hydrogen and iron within a wide temperature range of 700–2000 K at 5.0 GPa. Some crucial findings were obtained—(i) the mobility of hydrogen associated with Mg vacancy and Fe³⁺ defects change significantly with temperature; (ii) at high temperature, hydrogen is able to escape from the associated defect to form “free proton,” which is able to diffuse freely in olivine lattice shown high proton conductivity; (iii) the diffusion of ionized protons is highly anisotropic with extraordinary high diffusion coefficient along with [100] direction, and (V) hydrogen associated with Si vacancy is stable even at 2000 K. It suggests that different kind of hydrogen defect present different mobility at high temperature with great influence on ionic conductivity of hydrous olivine. AIMD simulations on hydrous wadsleyite and ringwoodite also suggest a higher diffusion rate of hydrogen at Mg vacancy in comparison with hydrogen at Si vacancy [108]. The migration barrier enthalpies of hydrogen along different lattice directions were calculated by using the climbing image nudged elastic band (CINEB) method [109]. The calculation results support the anisotropic diffusion behavior of hydrogen in hydrous olivine. The activation enthalpies for proton migration along with [100] direction in different models is about 180–240 kJ/mole, which is similar to the experimental results obtained by conductivity (140 ± 6 kJ/mole) and diffusion coefficient (229 ± 18 kJ/mole) measurements [13, 37]. Based on all of these obtained calculation results, an ionization-hopping proton conduction mechanism is proposed and the conductivity is calculated, as shown in **Figure 6**. Obviously, an approximately 80–160 ppm wt water content (correlated with Mg/Fe defects) in olivine is sufficient to produce the high and highly anisotropic conductivity anomaly ($\sim 10^{-1}$ S/m). The results are consistent with previous experimental studies and provide a good constraint on the conduction mechanism within an atomic scale for hydrous olivine. It also suggests previous conductivity measurements at relatively low temperatures ignored the contribution of ionized

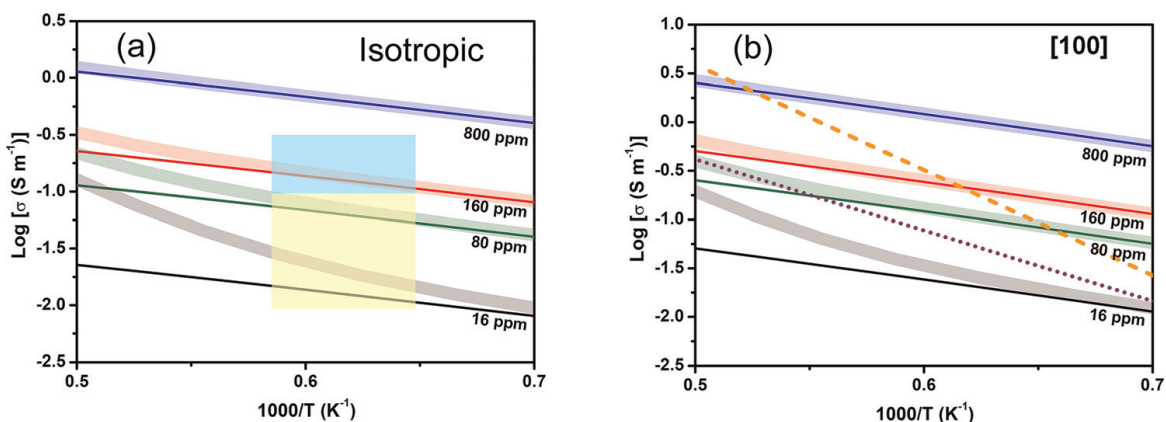


Figure 6.

The extrapolated proton and total conductivities of Fe-bearing hydrous olivine as the function of inverse temperature and water content compared with experimental results [13, 15, 110]. In here, the vertical axis stands for the logarithmic electrical conductivity (the corresponding unit is S/m) and the horizontal axis stands for the inverse temperature (the corresponding unit is Kelvin), respectively. The conductivities with 16, 80, 160, and 800 ppm wt water content associated with V_{Mg}'' or Fe^{3+} . Thick-light curves are the total conductivities counting on the measured conductivities of dry olivine [111]. Light yellow and cyan areas show the conductivity range representing conductivity structures at the asthenosphere (Reproduced with permission from He et al., *J. Geophys. Res. Solid Earth*; published by American Geophysical Union, 2121 [15]).

hydrogen, thus the extrapolated data underestimates the proton conduction for the electrical conductivity of hydrous olivine at high temperatures of the asthenosphere.

4.2 Electrical conductivity of pyroxene

As a secondary rock-forming mineral in the upper mantle, the volume percentage of pyroxene is close to the average content of 20–40% in a typical upper-mantle region. Thus, high-pressure electrical conductivity measurement on pyroxene is crucial to deeply explore the high conductivity anomalies in the regions of the upper mantle and mantle asthenosphere. For anhydrous clinopyroxene, Dai et al. [111] measured EC of dry single-crystal diopside along with [001, 010, 100] three main crystallographic orientations at 1.0–4.0 GPa, 1073–1373 K, and Ni-NiO oxygen buffer-controlled oxygen fugacity in the YJ-3000 t multi-anvil apparatus and the Solartron-1260 impedance spectroscopy analyzer. A feeble influence of anisotropy on the electrical conductivity of dry single-crystal diopside was observed. Similarly, the influence of oxygen fugacity on the electrical conductivity of dry orthopyroxene single crystal by Dai et al. [112] was performed at 1.0–4.0 GPa, 1073–1423 K, and different oxygen fugacities. The oxygen fugacity in the sample chamber of EC measurements is controlled by four solid buffers of nickel and nickel oxide, iron and magnetite, and as well as molybdenum and molybdenum dioxide. A positive dependence of oxygen fugacity on the EC of orthopyroxene single crystal is observed at a given temperature range from 1073 K to 1423 K and 2.0 GPa, which is highly related to the conduction mechanism of small polaron hopping in the anhydrous iron-bearing silicate mineral at high pressure.

On the other hand, EC measurements of anhydrous and hydrous orthopyroxene single crystals along with three main crystallographic orientations were performed by Dai and Karato [51] at conditions of 8 GPa, temperatures of 873–1273 K, and as well as the oxygen fugacity controlled by the molybdenum and molybdenum dioxide using the Kawai-1000 t multi-anvil apparatus and the Solartron-1260 impedance spectroscopy analyzer. Detailed experimental results were illustrated in **Figure 7**. According to

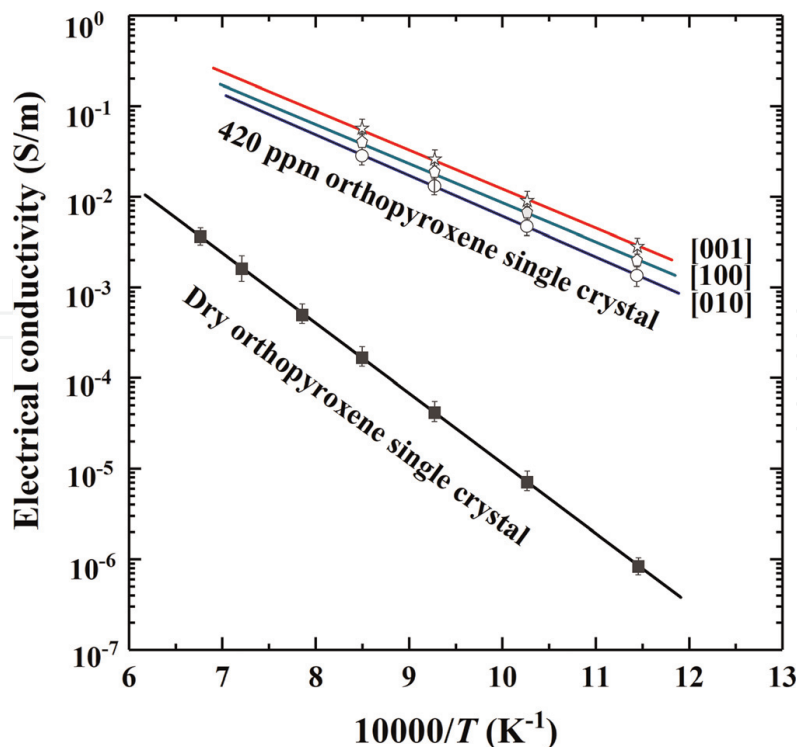


Figure 7.

The influence of anisotropy on the electrical conductivity of hydrous single-crystal orthopyroxene along [001, 010, 100] crystallographic orientations at conditions of 8 GPa, temperatures of 873–1273 K, and as well as the oxygen fugacity controlled by the molybdenum and molybdenum dioxide. The EC of dry single-crystal orthopyroxene is also included (modified from Dai and Karato [51]).

the FT-IR spectroscopy results, the hydrous orthopyroxene single crystals contain 420 ppm wt% water. They found that trace structural water can enhance several orders of magnitude in the EC of orthopyroxene single crystals. The effect from the anisotropy of hydrous orthopyroxene on the EC of the sample can be neglected, which is consistent with the above-mentioned dry single-crystal diopside. As two main conduction mechanisms, small polaron and free proton play a crucial role in the electrical conductivity of anhydrous and hydrous orthopyroxene single crystals at high-temperature and high-pressure conditions.

In the recent days, Sun et al. [27] performed electrical conductivities of the polycrystalline clinopyroxene aggregates + sodium chloride + water system under conditions of 1 GPa, 673–973 K, the various salinity degree of fluid (5, 10, 15, 20, and 25%), and the volume fraction of fluid (5, 10, 15, 20, and 25%) using the YJ-3000 t multi-anvil apparatus and the Solartron-1260 impedance spectroscopy analyzer. They found that the electrical conductivity of polycrystalline clinopyroxene aggregates containing the salinity-bearing fluid with a certain salinity degree and volume fraction of fluid can be applied to explain the unusually high conductivities in some regional geotectonic units, such as southern Tibetan plateau, Dabie orogen, Grenville province, and central New Zealand.

4.3 Electrical conductivity of garnet

As a type of important constituent silicate mineral, garnet can stably exist over a wide depth from lower crust Earth to the topmost lower mantle. With increasing temperature and pressure in the deep Earth interiors, the form of pyrope-rich garnet in the lower Earth crust gradually transforms into the high-pressure phase of majorite

garnet in the mantle transition zone, which is of the complex chemical composition and stable crystalline structure. Furthermore, the mineralogical content of garnet in the deep Earth interiors will gradually increase with the rise of depth [113]. Therefore, when we try to construct the profile between electrical conductivity and depth in the deep mantle of Earth's interior, it is indispensable to comprehensively assess the influence of electrical conductivity of garnet at high temperatures and high pressures.

Dai and Karato [52] conducted the EC measurements of anhydrous and water-rich single-crystal pyrope-rich garnet [its corresponding chemical composition is close to 73 mole% of pyrope (Py), 14 mole% of almandine (Alm), and 13 mole% of grossular (Gr)] at conditions of temperature range from 873 K to 1473 K, pressure ranges from 4 GPa to 16 GPa, frequency ranges from 10^{-2} Hz to 10^6 Hz and water-bearing content range from less than 10 H/10⁶Si to 7000 H/10⁶Si using the Kawai-1000 t multi-anvil press installed in the Karato High-pressure Laboratory, Department of Earth and Planetary Sciences, Yale University, United States. **Figure 8** shows the effect of pressure on the dry and water-bearing (160 ppm wt) single crystal pyrope-rich garnet at temperatures of 873–1473 K. In comparisons with water-free water of pyrope-rich garnet, the electrical conductivity of the hydrous sample is higher, and the activation enthalpy of pyrope-rich garnet ($\Delta H = \sim 70$ kJ/mole) is lower than that of the anhydrous sample ($\Delta H = \sim 128$ kJ/mole).

In subsequent investigations, a series of EC experiments on garnet with different chemical compositions (Py₂₀Alm₇₆Grs₄, Py₃₀Alm₆₇Grs₃, Py₅₆Alm₄₃Grs₁, Py₇₃Alm₁₄Grs₁₃, and Alm₈₂Py₁₅Grs₃) were conducted by Dai et al. [53, 54] using the YJ-3000 t multi-anvil apparatus and the Solartron-1260 impedance spectroscopy analyzer to explore the influences of oxygen fugacity and mineralogical composition on the EC of garnet at 1.0–4.0 GPa and 873–1273 K. Five different solid buffers including Fe₃O₄-Fe₂O₃, Ni-NiO, Fe-Fe₃O₄, Fe-FeO, and Mo-MoO₂ were employed to control the oxygen fugacity of the high-pressure sample chamber. Based on these obtained

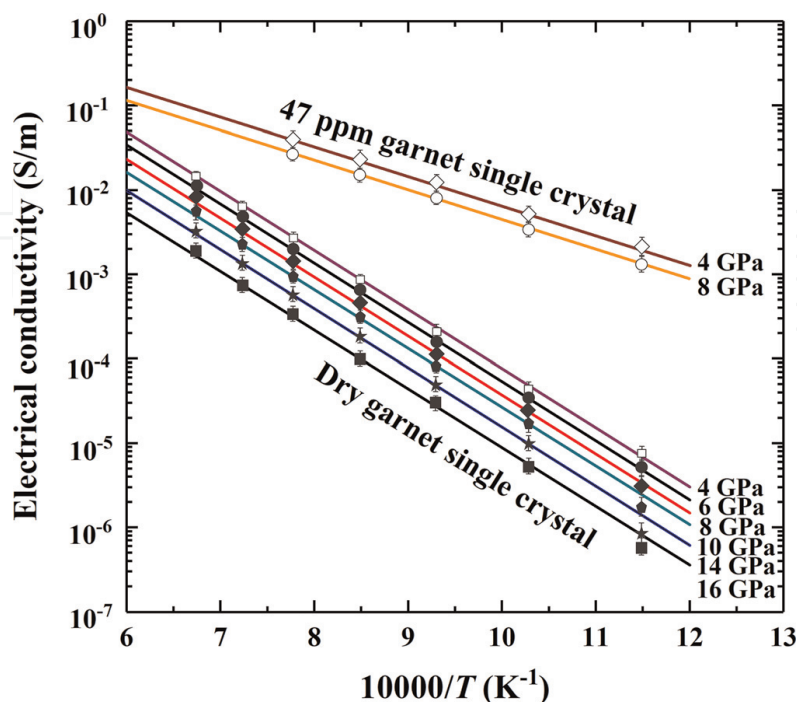


Figure 8.

*The influence of pressure on the dry and water-bearing (160 ppm wt) single crystal pyrope-rich garnet at temperatures of 873–1473 K (reproduced with permission from Dai and Karato, *Phys. Earth planet. Inter.*; published by Elsevier, 2009 [52]).*

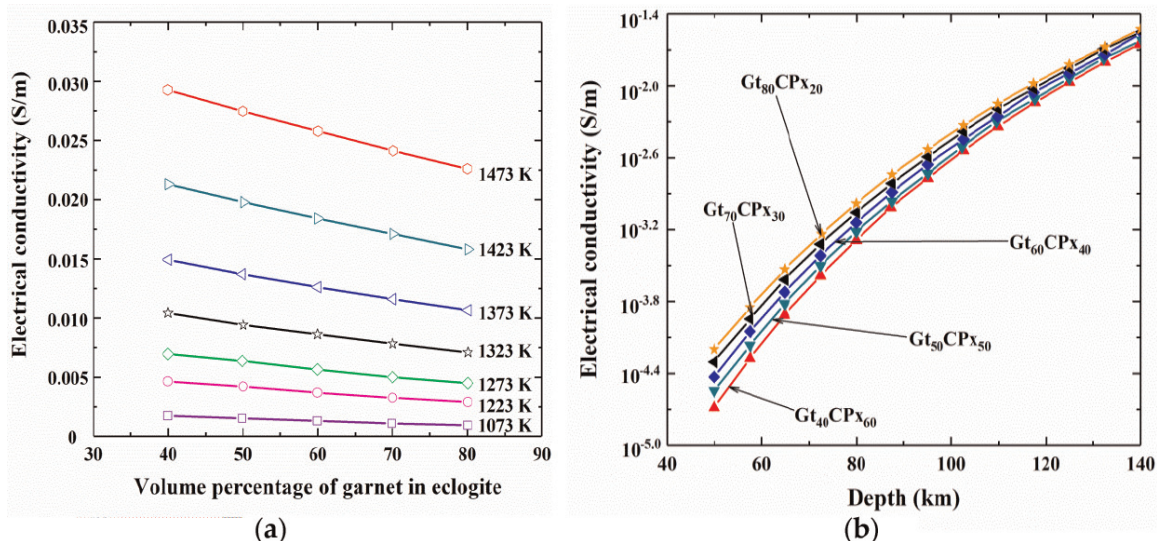


Figure 9. (a) The influence of volume percentage on the electrical conductivity of eclogite on the base on our obtained electrical conductivity results for single crystal pyrope-rich garnet at high temperatures and high pressures (modified from Dai et al. [53]), (b) the profile between the electrical conductivity of eclogite and depth in conjunction with previously available electrical conductivity of clinopyroxene results, the average models of rock and as well as the regionally geothermal gradient is established from the EC of garnet series at high temperatures and high pressures (reproduced with permission from Dai et al., *Contrib. Mineral. Petrol.*; published by Springer Nature, 2012 [53]).

experimental results, some absolutely new models of electrical conductivity of garnet series as functions of the variation of oxygen fugacity and chemical compositions have already been constructed, as illustrated in **Figure 9(a)** in detail. Furthermore, in conjunction with previously available electrical conductivity of clinopyroxene results, the average models of rock and as well as the regionally geothermal gradient, the profile between the electrical conductivity of eclogite and depth is established from the EC of garnet series at high temperatures and high pressures, as shown in **Figure 9(b)** in detail. All of these acquired laboratory-based electrical conductivity profiles can be widely applied to systematically disclose and deeply explore the cause of the observable high conductivity anomalies from global and regional field magnetotelluric and geomagnetic deep sounding results in those representatively geotectonic units, for example, stable mid-lower continental Earth crust, Dabie-Sulu ultrahigh-pressure metamorphic belt of eastern China, Tibet plateau, and North China craton.

5. Conclusions

High-pressure laboratory-based measurement results on electrical properties of several dominant minerals (olivine, orthopyroxene, clinopyroxene, garnet, etc.) in the upper mantle regions are highly sensitive to some influential factors including temperature, pressure, oxygen fugacity, water content, crystallographic orientation, trace element of titanium content and iron content. The proper determination of EC of upper-mantle minerals in a broad temperature and pressure range requires the utilization of complex electrical electrochemical impedance spectroscopy measurements. The iron-related hopping of small polaron and the hydrogen-related defects are possibly the two dominant conduction mechanisms in anhydrous and hydrous Fe-bearing silicate minerals within the depth range of the upper mantle. The trace structural water of mantle minerals plays a crucial role in explaining the high conductivity

anomaly and the water distribution in the deep mantle. In comprehensive considerations of some newest results from high-pressure laboratory-based conductivity measurements, geophysical field observations, and first-principles theoretical calculations, high and highly anisotropic EC at the corresponding asthenospheric temperature and pressure conditions can be used to reasonably explain by the 100 ppm wt% of water content for the high conductivity anomaly in the asthenospheric region. In addition, the influence of the interconnected high conductive impurity phases (graphite, magnetite, chromite, sulfide impurity, etc.) and saline fluids (e.g., Ol-NaCl-H₂O, Ol-KCl-H₂O, Ol-CaCl₂-H₂O, etc.) on the EC of olivine also needed to be considered in a special geotectonic environment. With the development and advancement of measurement techniques and experimental methods, more and more laboratory-based high-pressure conductivity experimental results will be indispensable to systematically disclose the cycle discontinuity and high conductivity anomaly in the upper-mantle region.

Acknowledgements


Almost all listed original high-pressure electrical conductivity data have already been obtained by Lidong Dai and his collaborators in the Chinese Academy of Sciences and Yale University. In here, please accept my best honest thanks and greetings to Professor Heping Li in the Key Laboratory of High-temperature and High-pressure Study of the Earth's Interior (HTHPSEI), Institute of Geochemistry, Chinese Academy of Sciences, the People's Republic of China, and Professor Shun-ichiro Karato in the Karato High-pressure Laboratory, Department of Earth and Planetary Sciences, Yale University, United States. This work was financially supported by the National Natural Science Foundation of China (Grant numbers 42072055, 41774099, and 41772042), Youth Innovation Promotion Association of Chinese Academy of Sciences (Grant number 2019390), Special Fund of the West Light Foundation of Chinese Academy of Sciences and as well as Special Fund from Shandong Provincial Key Laboratory of Water and Soil Conservation and Environmental Protection.

Author details

Lidong Dai*, Haiying Hu*, Yu He and Wenqing Sun
Key Laboratory of High-Temperature and High-Pressure Study of the Earth's Interior,
Institute of Geochemistry, Chinese Academy of Sciences, Guiyang, Guizhou, China

*Address all correspondence to: dailidong@vip.gyig.ac.cn; huhaiying@vip.gyig.ac.cn

IntechOpen

© 2022 The Author(s). Licensee IntechOpen. This chapter is distributed under the terms of the Creative Commons Attribution License (<http://creativecommons.org/licenses/by/3.0>), which permits unrestricted use, distribution, and reproduction in any medium, provided the original work is properly cited. 

References

- [1] Yang B, Egbert G, Zhang H, Meqbel N, Hu X. Electrical resistivity imaging of continental United States from three-dimensional inversion of EarthScope USArray magnetotelluric data. *Earth and Planetary Science Letters*. 2021;**576**: 117244. DOI: 10.1016/j.epsl.2021.117244
- [2] Förster M, Selway K. Melting of subducted sediments reconciles geophysical images of subduction zones. *Nature Communications*. 2021;**12**:1-7
- [3] Dai L, Karato S. Electrical conductivity of wadsleyite at high temperatures and high pressures. *Earth and Planetary Science Letters*. 2009;**287**:277-283
- [4] Dai L, Hu H, Li H, Wu L, Hui K, Jiang J, et al. Influence of temperature, pressure, and oxygen fugacity on the electrical conductivity of dry eclogite, and geophysical implications. *Geochemistry, Geophysics, Geosystems*. 2016;**17**:2394-2407
- [5] Dai L, Hu H, Jiang J, Sun W, Li H, Wang M, et al. An overview of the experimental studies on the electrical conductivity of major minerals in the upper mantle and transition zone. *Materials*. 2020;**13**:408. DOI: 10.3390/ma13020408
- [6] Hu H, Li H, Dai L, Shan S, Zhu C. Electrical conductivity of albite at high temperatures and high pressures. *American Mineralogist*. 2011;**96**: 1821-1827
- [7] Hu H, Li H, Dai L, Shan S, Zhu C. Electrical conductivity of alkali feldspar solid solutions at high temperatures and high pressures. *Physics and Chemistry of Minerals*. 2013;**40**:51-62
- [8] Dai L, Karato S. Electrical conductivity of Ti-bearing hydrous olivine aggregates at high temperature and high pressure. *Journal of Geophysical Research—Solid Earth*. 2020;**125**:e2020JB020309. DOI: 10.1029/2020JB020309
- [9] Lin J, Weir S, Jackson D, Evans W, Vohra Y, Qiu W, et al. Electrical conductivity of the lower-mantle ferropericlase across the electronic spin transition. *Geophysical Research Letters*. 2007;**34**:L16305. DOI: 10.1029/2007GL030523
- [10] Ohta K, Onoda S, Hirose K, Sinmyo R, Shimizu K, Sata N, et al. The electrical conductivity of post-perovskite in Earth's D" layer. *Science*. 2008;**320**: 89-91
- [11] Wang D, Li H, Yi L, Matsuzaki T, Yoshino T. Anisotropy of synthetic quartz electrical conductivity at high pressure and temperature. *Journal of Geophysical Research—Solid Earth*. 2010;**115**:B09211. DOI: 10.1029/2009JB006695
- [12] Guo X, Yoshino T, Katayama I. Electrical conductivity anisotropy of deformed talc rocks and serpentinites at 3 GPa. *Physics of the Earth and Planetary Interiors*. 2011;**188**:69-81
- [13] Dai L, Karato S. High and highly anisotropic electrical conductivity of the asthenosphere due to hydrogen diffusion in olivine. *Earth and Planetary Science Letters*. 2014;**408**:79-86
- [14] Dai L, Karato S. Reply to comment on "High and highly anisotropic electrical conductivity of the asthenosphere due to hydrogen diffusion in olivine" by Dai and Karato [*Earth Planet. Sci. Lett.* 408 (2014) 79–86]. *Earth and Planetary Science Letters*. 2015;**427**:300-302

- [15] He Y, Dai L, Kim D, Li H, Karato S. Thermal ionization of hydrogen in hydrous olivine with enhanced and anisotropic conductivity. *Journal of Geophysical Research—Solid Earth*. 2021;**126**:e2021JB022939. DOI: 10.1029/2021JB022939
- [16] Huang X, Xu Y, Karato S. Water content in the transition zone from electrical conductivity of wadsleyite and ringwoodite. *Nature*. 2005;**434**:746-749
- [17] Wang D, Mookherjee M, Xu Y, Karato S. The effect of water on the electrical conductivity of olivine. *Nature*. 2006;**443**:977-980
- [18] He Y, Hou M, Jang B, Sun S, Zhuang Y, Deng L, et al. Superionic iron oxide–hydroxide in Earth's deep mantle. *Nature Geoscience*. 2021;**14**:174-178
- [19] Manthilake M, Matsuzaki T, Yoshino T, Yamashita S, Ito E, Katsura T. Electrical conductivity of wadsleyite as a function of temperature and water content. *Physics of the Earth and Planetary Interiors*. 2009;**174**:10-18
- [20] Pommier A, Leinenweber K, Tasaka M. Experimental investigation of the electrical behavior of olivine during partial melting under pressure and application to the lunar mantle. *Earth and Planetary Science Letters*. 2015;**425**:242-255
- [21] Yoshino T, Matsuzaki T, Yamashita S, Katsura T. Hydrous olivine unable to account for conductivity anomaly at the top of the asthenosphere. *Nature*. 2006;**443**:973-976
- [22] Hu H, Dai L, Li H, Hui K, Sun W. Influence of dehydration on the electrical conductivity of epidote and implications for high-conductivity anomalies in subduction zones. *Journal of Geophysical Research—Solid Earth*. 2017;**122**:2751-2762
- [23] Sun W, Dai L, Li H, Hu H, Wu L, Jiang J. Electrical conductivity of mudstone (before and after dehydration at high PT) and a test of high conductivity layers in the crust. *American Mineralogist*. 2017;**102**:2450-2456
- [24] Hu H, Dai L, Li H, Sun W, Li B. Effect of dehydrogenation on the electrical conductivity of Fe-bearing amphibole: Implications for high conductivity anomalies in subduction zones and continental crust. *Earth and Planetary Science Letters*. 2018;**498**:27-37
- [25] Dai L, Hu H, Sun W, Li H, Liu C, Wang M. Influence of high conductive magnetite impurity on the electrical conductivity of dry olivine aggregates at high temperature and high pressure. *Minerals*. 2019;**9**:44. DOI: 10.3390/min9010044
- [26] Sun W, Jiang J, Dai L, Hu H, Wang M, Qi Y, et al. Electrical properties of dry polycrystalline olivine mixed with various chromite contents: Implications for the high-conductivity anomalies in subduction zones. *Geoscience Frontiers*. 2021;**12**:101178. DOI: 10.1016/j.gsf.2021.101178
- [27] Sun W, Dai L, Li H, Hu H, Jiang J, Wang M. Electrical conductivity of clinopyroxene-NaCl-H₂O system at high temperatures and pressures: Implications for high-conductivity anomalies in the deep crust and subduction zone. *Journal of Geophysical Research—Solid Earth*. 2020;**125**:e2019JB019093. DOI: 10.1029/2019JB019093
- [28] Sun W, Dai L, Hu H, Jiang J, Wang M, Hu Z, et al. Influence of saline fluids on the electrical conductivity of

olivine aggregates at high temperature and high pressure and its geological implications. *Frontiers in Earth Science*. 2021;**9**:749896. DOI: 10.3389/feart.2021.749896

[29] Dai L, Pu C, Li H, Hu H, Liu K, Yang L, et al. Characterization of metallization and amorphization for GaP under different hydrostatic environments in diamond anvil cell up to 40.0 GPa. *The Review of Scientific Instruments*. 2019;**90**:066103. DOI: 10.1063/1.5093949

[30] Dai L, Liu K, Li H, Wu L, Hu H, Zhuang Y, et al. Pressure-induced irreversible metallization with phase transitions of Sb_2S_3 . *Physical Review B*. 2018;**97**:024103. DOI: 10.1103/PhysRevB.97.024103

[31] Dai L, Zhuang Y, Li H, Wu L, Hu H, Liu K, et al. Pressure-induced irreversible amorphization and metallization with a structural phase transition in arsenic telluride. *Journal of Materials Chemistry C*. 2017;**5**:12157-12162

[32] Hong M, Dai L, Hu H, Yang L and Zhang X. Pressure-induced structural phase transitions in natural kaolinite investigated by Raman spectroscopy and electrical conductivity. *American Mineralogist*. 2022. In press. DOI: 10.2138/am-2021-7863

[33] Yang L, Dai L, Li H, Hu H, Hong M, Zhang X, et al. High-pressure investigations on the isostructural phase transition and metallization in realgar with diamond anvil cells. *Geoscience Frontiers*. 2021;**12**:1031-1037

[34] Yang L, Jiang J, Dai L, Hu H, Hong M, Zhang X, et al. High-pressure structural phase transition and metallization in Ga_2S_3 under non-hydrostatic and hydrostatic conditions

up to 36.4 GPa. *Journal of Materials Chemistry C*. 2021;**9**:2912-2918

[35] Freitas D, Manthilake G. Electrical conductivity of hydrous silicate melts: Implications for the bottom-up hydration of Earth's upper mantle. *Earth and Planetary Science Letters*. 2019;**523**:115712. DOI: 10.1016/j.epsl.2019.115712

[36] Fei H, Wiedenbeck M, Yamazaki D, Katsura T. Small effect of water on upper-mantle rheology based on silicon self-diffusion coefficients. *Nature*. 2013;**498**:213-216

[37] Novella D, Jacobsen B, Weber P, Tyburczy J, Ryerson F, Du Frane W. Hydrogen self-diffusion in single crystal olivine and electrical conductivity of the Earth's mantle. *Scientific Reports*. 2017;**7**:5344. DOI: 10.1038/s41598-017-05113-6

[38] Jung H, Karato S. Water-induced fabric transitions in olivine. *Science*. 2001;**293**:1460-1463

[39] Kang H, Jung H. Lattice-preferred orientation of amphibole, chlorite, and olivine found in hydrated mantle peridotites from Bjørkedalen, southwestern Norway, and implications for seismic anisotropy. *Tectonophysics*. 2019;**750**:137-152

[40] Wei S, Wiens D, Zha Y, Plank T, Webb S, Blackman D, et al. Seismic evidence of effects of water on melt transport in the Lau back-arc mantle. *Nature*. 2015;**518**:395-398

[41] Cline IIC, Faul U, David E, Berry A, Jackson I. Redox-influenced seismic properties of upper-mantle olivine. *Nature*. 2018;**555**:355-358

[42] Nishihara Y, Maruyama G, Nishi M. Growth kinetics of forsterite reaction rims at high-pressure. *Physics of the*

Earth and Planetary Interiors. 2016;**257**: 220-229

[43] Cerpa N, Wada I, Wilson C. Fluid migration in the mantle wedge: Influence of mineral grain size and mantle compaction. *Journal of Geophysical Research—Solid Earth*. 2017;**122**:6247-6268

[44] Masotta M, Mollo S, Nazzari M, Tecchiato V, Scarlato P, Papale P, et al. Crystallization and partial melting of rhyolite and felsite rocks at Krafla volcano: A comparative approach based on mineral and glass chemistry of natural and experimental products. *Chemical Geology*. 2018;**483**:603-618

[45] Peslier A, Hervig R, Yang S, Humayun M, Barnes J, Irving A, et al. Determination of the water content and D/H ratio of the Martian mantle by unraveling degassing and crystallization effects in nakhlites. *Geochimica et Cosmochimica Acta*. 2019;**266**:382-415

[46] Karato S. The role of hydrogen in the electrical conductivity of the upper mantle. *Nature*. 1990;**347**:272-273

[47] Dai L, Karato S. Influence of FeO and H on the electrical conductivity of olivine. *Physics of the Earth and Planetary Interiors*. 2014;**237**:73-79

[48] Dai L, Karato S. Influence of oxygen fugacity on the electrical conductivity of hydrous olivine: Implications for the mechanism of conduction. *Physics of the Earth and Planetary Interiors*. 2014;**232**: 57-60

[49] Dai L, Karato S. The effect of pressure on the electrical conductivity of olivine under the hydrogen-rich conditions. *Physics of the Earth and Planetary Interiors*. 2014;**232**:51-56

[50] Katsura T, Baba K, Yoshino T, Kogiso T. Electrical conductivity of the

oceanic asthenosphere and its interpretation based on laboratory measurements. *Tectonophysics*. 2017; **717**:162-181

[51] Dai L, Karato S. Electrical conductivity of orthopyroxene: Implications for the water content of the asthenosphere. *Proceedings of the Japan Academy*. 2009;**85**:466-475

[52] Dai L, Karato S. Electrical conductivity of pyrope-rich garnet at high temperature and high pressure. *Physics of the Earth and Planetary Interiors*. 2009;**176**:83-88

[53] Dai L, Li H, Hu H, Shan S, Jiang J, Hui K. The effect of chemical composition and oxygen fugacity on the electrical conductivity of dry and hydrous garnet at high temperatures and pressures. *Contributions to Mineralogy and Petrology*. 2012;**163**:689-700

[54] Dai L, Li H, Hu H, Jiang J, Hui K, Shan S. Electrical conductivity of $\text{Alm}_{82}\text{Py}_{15}\text{Grs}_3$ almandine-rich garnet determined by impedance spectroscopy at high temperatures and high pressures. *Tectonophysics*. 2013;**608**:1086-1093

[55] Xu Y, Poe B, Shankland T, Rubie D. Electrical conductivity of olivine, wadsleyite, and ringwoodite under upper-mantle conditions. *Science*. 1998; **280**:1415-1418

[56] Xu Y, McCammon C, Poe B. The effect of alumina on the electrical conductivity of silicate perovskite. *Science*. 1998;**282**:922-924

[57] Poe B, Xu Y. In situ complex impedance spectroscopy of mantle minerals measured at 20 GPa and 1400 °C. *Phase Transitions*. 1999;**68**:453-466

[58] Xu Y, Shankland T. Electrical conductivity of orthopyroxene and its

high pressure phases. *Geophysical Research Letters*. 1999;**26**:2645-2648

[59] Xu Y, Shankland T, Poe B. Laboratory-based electrical conductivity in the Earth's mantle. *Journal of Geophysical Research—Solid Earth*. 2000;**105**:27865-27875

[60] Xu Y, Shankland T, Duba A. Pressure effect on electrical conductivity of mantle olivine. *Physics of the Earth and Planetary Interiors*. 2000;**118**:149-161

[61] Laštovičková M. Laboratory measurements of electrical properties of rocks and minerals. *Geophysical Surveys*. 1983;**6**:201-213

[62] Roberts J, Tyburczy J. Frequency dependent electrical properties of polycrystalline olivine compacts. *Journal of Geophysical Research*. 1991;**96**:16205-16222

[63] Nover G. Electrical properties of crustal and mantle rocks—A review of laboratory measurements and their explanation. *Surveys in Geophysics*. 2005;**26**:593-651

[64] Yoshino T. Laboratory electrical conductivity measurement of mantle minerals. *Surveys in Geophysics*. 2010;**31**:163-206

[65] Saltas V, Vallianatos F, Gidaracos E. Charge transport in diatomaceous earth studied by broadband dielectric spectroscopy. *Applied Clay Science*. 2013;**80–81**:226-235

[66] Vallianatos F, Saltas V. Application of the $cB\Omega$ model to the calculation of diffusion parameters of He in olivine. *Physics and Chemistry of Minerals*. 2014;**41**:181-188

[67] Karato S, Wang D. Electrical conductivity of minerals and rocks. In:

Physics and Chemistry of the Deep Earth, 1st ed. John Wiley & Sons, Ltd: Hoboken, NJ, USA; 2013

[68] Pommier A, Leinenweber K. Electrical cell assembly for reproducible conductivity experiments in the multi-anvil. *American Mineralogist*. 2018;**103**:1298-1305

[69] Xie H. *Introduction to Science of the Earth Interior Material*. Beijing, China: Peking Science Press; 1997

[70] Zheng H, Xie H, Xu Y, Song M, Guo J, Zhang Y. The electrical conductivity of H₂O at 0.21–4.18 GPa and 20–350 °C. *Scientific Bulletin*. 1997;**42**:969-976

[71] Zheng H, Xie H, Xu Y, Song M, Guo J, Zhang Y. Measurement of electrical conductivity of 0.001 mol NaCl solution under high pressures. *Scientific Bulletin*. 1997;**42**:1563-1566

[72] Wang D, Li H, Yi L, Shi B. The electrical conductivity of upper-mantle rocks: Water content in the upper mantle. *Physics and Chemistry of Minerals*. 2008;**35**:157-162

[73] Wang D, Guo Y, Yu Y, Karato S. Electrical conductivity of amphibole-bearing rocks: Influence of dehydration. *Contributions to Mineralogy and Petrology*. 2012;**164**:17-25

[74] Dai L, Li H, Liu C, Su G, Shan S. Experimental measurement on the electrical conductivity of pyroxenite at high temperature and high pressure under different oxygen fugacities. *High Pressure Research*. 2006;**26**:193-202

[75] Dai L, Li H, Deng H, Liu C, Su G, Shan S, et al. In-situ control of different oxygen fugacity experimental study on the electrical conductivity of lherzolite at

high temperature and high pressure. *Journal of Physics and Chemistry of Solids*. 2008;**69**:101-110

[76] Dai L, Li H, Li C, Hu H, Shan S. The electrical conductivity of dry polycrystalline olivine compacts at high temperatures and pressures. *Mineralogical Magazine*. 2010;**74**: 849-857

[77] Dai L, Hu H, Li H, Jiang J, Hui K. Influence of temperature, pressure, and chemical composition on the electrical conductivity of granite. *American Mineralogist*. 2014;**99**:1420-1428

[78] Dai L, Hu H, Li H, Hui K, Jiang J, Li J, et al. Electrical conductivity of gabbro: The effects of temperature, pressure and oxygen fugacity. *European Journal of Mineralogy*. 2015;**27**:215-224

[79] Dai L, Jiang J, Li H, Hu H, Hui K. Electrical conductivity of hydrous natural basalt at high temperatures and high pressures. *Journal of Applied Geophysics*. 2015;**112**:290-297

[80] Dai L, Sun W, Li H, Hu H, Wu L, Jiang J. Effect of chemical composition on the electrical conductivity of gneiss at high temperatures and pressures. *Solid Earth*. 2018;**9**:233-245

[81] Hu H, Dai L, Li H, Jiang J, Hui K. Electrical conductivity of K-feldspar at high temperature and high pressure. *Mineralogy and Petrology*. 2014;**108**: 609-618

[82] Hu H, Dai L, Li H, Hui K, Li J. Temperature and pressure dependence of electrical conductivity in synthetic anorthite. *Solid State Ionics*. 2015;**276**: 136-141

[83] Hui K, Zhang H, Li H, Dai L, Hu H, Jiang J, et al. Experimental study on the electrical conductivity of quartz andesite

at high temperature and high pressure: Evidence of grain boundary transport. *Solid Earth*. 2015;**6**:1037-1043

[84] Hui K, Dai L, Li H, Hu H, Jiang J, Sun W, et al. Experimental study on the electrical conductivity of pyroxene andesite at high temperature and high pressure. *Pure and Applied Geophysics*. 2017;**174**:1033-1041

[85] Sun W, Dai L, Li H, Hu H, Jiang J, Hui K. Effect of dehydration on the electrical conductivity of phyllite at high temperatures and pressures. *Mineralogy and Petrology*. 2014;**111**:853-863

[86] Sun W, Dai L, Li H, Hu H, Liu C. Effect of temperature, pressure and chemical composition on the electrical conductivity of granulite and geophysical implications. *Journal of Mineralogical and Petrological Sciences*. 2019;**114**:87-98

[87] Sun W, Dai L, Li H, Hu H, Liu C, Wang M. Effect of temperature, pressure and chemical compositions on the electrical conductivity of schist: Implications for electrical structures under the Tibetan plateau. *Materials*. 2019;**12**:961. DOI: 10.3390/ma12060961

[88] Dai L, Li H, Hu H, Shan S. Experimental study of grain boundary electrical conductivities of dry synthetic peridotite under high-temperature, high-pressure, and different oxygen fugacity conditions. *Journal of Geophysical Research—Solid Earth*. 2008;**113**:B12211. DOI: 10.1029/2008JB005820

[89] Dai L, Li H, Hu H, Shan S. Novel technique to control oxygen fugacity during high-pressure measurements of grain boundary conductivities of rocks. *The Review of Scientific Instruments*. 2009;**80**:033903. DOI: 10.1063/1.3097882

- [90] Dai L, Li H, Hu H, Shan S. In-situ control of oxygen fugacity for laboratory measurements of electrical conductivity of minerals and rocks in multi-anvil press. *Chinese Physics B*. 2011;**20**:049101. DOI: 10.1088/1674-1056/20/4/049101
- [91] Dai L, Hu H, Li H, Sun W, Jiang J. Influence of anisotropy on the electrical conductivity and diffusion coefficient of dry K-feldspar: Implications for the mechanism of conduction. *Chinese Physics B*. 2018;**27**:028703. DOI: 10.1088/1674-1056/27/2/028703
- [92] Xu J, Zhang Y, Hou W, Xu H, Guo J, Wang Z, et al. Measurements of ultrasonic wave velocities at high temperature and high pressure for window glass, pyrophyllite, and kimberlite up to 1400 °C and 5.5 GPa. *High Temperatures—High Pressures*. 1994;**26**:375-384
- [93] Liu Y, Xie H, Zhou W, Guo J. A method for experimental determination of compressional velocities in rocks and minerals at high pressure and high temperature. *Journal of Physics. Condensed Matter*. 2002;**14**:11381-11384
- [94] Xie H, Zhou W, Zhu M, Liu Y, Zhao Z, Guo J. Elastic and electrical properties of serpentinite dehydration at high temperature and high pressure. *Journal of Physics. Condensed Matter*. 2002;**14**:11359-11363
- [95] Song W, Liu Y, Wang Z, Gong C, Guo J, Zhou W, et al. Measurement method for sound velocity of melts in large volume press and its application to liquid sodium up to 2.0 GPa. *The Review of Scientific Instruments*. 2011;**82**:086108. DOI: 10.1063/1.3625267
- [96] Zhou W, Fan D, Liu Y, Xie H. Measurements of wave velocity and electrical conductivity of an amphibolite from southwestern margin of the Tarim Basin at pressures to 1.0 GPa and temperatures to 700 °C: Comparison with field observations. *Geophysical Journal International*. 2011;**187**:1393-1404
- [97] Miao S, Li H, Chen G. The temperature dependence of thermal conductivity for lherzolites from the North China Craton and the associated constraints on the thermodynamic thickness of the lithosphere. *Geophysical Journal International*. 2014;**197**:900-909
- [98] Miao S, Li H, Chen G. Temperature dependence of thermal diffusivity, specific heat capacity, and thermal conductivity for several types of rocks. *Journal of Thermal Analysis and Calorimetry*. 2014;**115**:1057-1063
- [99] Miao S, Zhou Y, Li H. Thermal diffusivity of lherzolite at high pressures and high temperatures using pulse method. *Journal of Earth Science*. 2019;**30**:218-222
- [100] Zhang B, Hu X, Asimow P, Zhang X, Xu J, Fan D, et al. Crystal size distribution of amphibole grown from hydrous basaltic melt at 0.6–2.6 GPa and 860–970 °C. *American Mineralogist*. 2019;**104**:525-535
- [101] Yang X. Orientation-related electrical conductivity of hydrous olivine, clinopyroxene and plagioclase and implications for the structure of the lower continental crust and uppermost mantle. *Earth and Planetary Science Letters*. 2012;**317**:241-250
- [102] Poe B, Romano C, Nestola F, Smyth J. Electrical conductivity anisotropy of dry and hydrous olivine at 8 GPa. *Physics of the Earth and Planetary Interiors*. 2010;**181**:103-111
- [103] Karato S. Some remarks on hydrogen-assisted electrical conductivity

in olivine and other minerals. *Progress in Earth and Planetary Science*. 2019;**6**:55. DOI: 10.1186/s40645-019-0301-2

[104] Du Frane W, Tyburczy J. Deuterium–hydrogen interdiffusion in olivine: Implications for point defects and electrical conductivity. *Geochemistry, Geophysics, Geosystems*. 2012;**13**:Q03004. DOI: 10.1029/2011GC003895

[105] Watson H, Roberts J, Tyburczy J. Effect of conductive impurities on electrical conductivity in polycrystalline olivine. *Geophysical Research Letters*. 2010;**37**:L02302. DOI: 10.1029/2009GL041566

[106] Wang D, Karato S, Jiang Z. An experimental study of the influence of graphite on the electrical conductivity of olivine aggregates. *Geophysical Research Letters*. 2013;**40**:2028-2032

[107] Huang Y, Guo H, Nakatani T, Uesugi K, Nakamura M, Keppler H. Electrical conductivity in texturally equilibrated fluid-bearing forsterite aggregates at 800 °C and 1 GPa: Implications for the high electrical conductivity anomalies in mantle wedges. *Journal of Geophysical Research—Solid Earth*. 2021;**126**:e2020JB021343. DOI: 10.1029/2020JB021343

[108] Caracas R, Panero W. Hydrogen mobility in transition zone silicates. *Progress in Earth and Planetary Science*. 2017;**4**:9. DOI: 10.1186/s40645-017-0119-8

[109] Henkelman G, Uberuaga B, Jonsson H. A climbing image nudged elastic band method for finding saddle points and minimum energy paths. *The Journal of Chemical Physics*. 2000;**113**:9901-9904

[110] Gardés E, Gaillard F, Tarits P. Toward a unified hydrous olivine

electrical conductivity law. *Geochemistry, Geophysics, Geosystems*. 2014;**15**:4984-5000

[111] Dai L, Li H, Liu C, Shan S, Cui T, Su G. Experimental study on the electrical conductivity of orthopyroxene at high temperature and high pressure under different oxygen fugacities. *Acta Geologica Sinica—English Edition*. 2005;**79**:803-809

[112] Dai L, Li H, Liu C, Su G, Cui T. In situ control of oxygen fugacity experimental study on the crystallographic anisotropy of the electrical conductivities of diopside at high temperature and high pressure. *Acta Petrologica Sinica*. 2005;**21**:1737-1742

[113] Yoshino T, Nishi M, Matsuzaki T, Yamazaki D, Katsura T. Electrical conductivity of majorite garnet and its implications for electrical structure in the mantle transition zone. *Physics of the Earth and Planetary Interiors*. 2008;**170**:193-200